INSTITUTE OF PHYSICS PUBLISHING JOURNAL OF PHYSICS B: ATOMIC, MOLECULAR AND OPTICAL PHYSICS

J. Phys. B: At. Mol. Opt. Phys. **36** (2003) 599–612 PII: S0953-4075(03)54725-3

Towards quantum information with trapped ions at NIST

D Leibfried[1,2], B DeMarco[1], V Meyer[1], M Rowe[3], A Ben-Kish[4], M Barrett[1], J Britton[1], J Hughes[5], W M Itano[1], B M Jelenković[6], C Langer[1], D Lucas[7], T Rosenband[1] and D J Wineland[1]

[1] Time and Frequency Division, NIST, Boulder, CO, USA
[2] Physics Department, University of Colorado, Boulder, CO, USA
[3] Optoelectronics Division, NIST, Boulder, CO, USA
[4] Department of Physics, Technion, Haifa, Israel
[5] Department of Physics, University of Virginia, VA, USA
[6] Institute of Physics, Belgrade, Yugoslavia
[7] Department of Physics, Oxford University, UK

Received 9 October 2002
Published 27 January 2003
Online at stacks.iop.org/JPhysB/36/599

Abstract

We report experiments on coherent quantum-state synthesis and the control of trapped atomic ions. This work has the overall goal of performing large-scale quantum information processing; however, such techniques can also be applied to fundamental tests and demonstrations of quantum mechanical principles, as well as to the improvement of quantum-limited measurements.

1. Introduction

Efforts to experimentally realize the elements of quantum computation (QC) via the use of trapped atomic ions have been stimulated, to a large extent, by the 1995 paper by Cirac and Zoller [1]. In this scheme, ions confined in a linear RF (Paul) trap are cooled and form a stable spatial array whose motion is described by normal modes. Two internal levels in each ion form a qubit (referred to as a spin qubit in what follows). Typically, the spacing between ions (>1 μm) is large enough that the direct coupling of internal states of two ions is negligible, thereby precluding logic gates based on internal-state interactions[8]. Cirac and Zoller [1] suggested cooling the ions to their motional ground state and using the ground and first excited states of a particular motional mode as a qubit (motion qubit). The motional mode can act as a data bus to transfer information between ions by first mapping the spin qubit state of a particular ion onto the selected motion qubit by the use of a laser beam focused onto that ion. Being able to perform logic gates between the motion qubit and another selected spin

[8] 'Dipole blockade' gates [2] based on Rydberg states as envisioned for neutral atoms are a possibility, but these gates are experimentally more challenging for ions because of the higher energies between the ground and Rydberg levels.

qubit, coupled with the ability to perform single spin qubit rotations, provides the basis for universal QC [3, 4].

The ion-trap scheme satisfies the main requirements for a quantum computer as outlined by DiVincenzo [5]:

(1) a scalable system of well-defined qubits,
(2) a method to reliably initialize the quantum system,
(3) long coherence times,
(4) the existence of universal gates, and
(5) an efficient measurement scheme.

Most of these requirements have been demonstrated experimentally; consequently, ion-trap quantum processors are studied in several laboratories. Here, we focus on experiments carried out at NIST but note that similar work is being pursued at Aarhus, Almaden (IBM), Hamburg, Hamilton (Ontario, McMaster University), Innsbruck, Los Alamos (LANL), University of Michigan, Garching (MPI), Oxford and Teddington (National Physical Laboratory, UK). For brevity, we discuss only recent experimental work on a proposed architecture towards scaling ion trap quantum information processing to a large system [6, 7], quantum simulation and quantum logic gates.

2. Multiplexed trap architecture

Although simple operations between a few ion qubits have been demonstrated, a viable quantum computer must look towards scaling to very large numbers of qubits. As the number of ions in a trap increases, several difficulties are encountered. For example, the addition of each ion adds three vibrational modes. It soon becomes nearly impossible to spectrally isolate the desired vibrational mode unless the speed of operations is slowed to undesirable levels [6, 8]. Furthermore, since error correction will most likely be incorporated into any large processor, it will be desirable to measure and reset ancilla qubits without disturbing the coherence of logical qubits. Since ion qubits are typically measured by means of state-dependent laser scattering, the scattered light from ancilla qubits held in a common trap may disturb the coherence of the logical qubits.

For these and other reasons, it appears that a scalable ion-trap system must incorporate arrays of interconnected traps, each holding a small number of ions. The information carriers between traps might be photons [9–11], or ions that are moved between traps in the array. In the latter case, a 'head' ion held in a movable trap could carry the information by moving from site to site as in the proposal given in [12]. Similarly, as has been proposed at NIST, we could shuttle ions around in an array of interconnected traps [6, 7]. In this last scheme, the idea is to move ions between nodes in the array by applying time-dependent potentials to 'control' electrode segments. To perform logic operations between selected ions, these ions are transferred into an 'accumulator' trap for the gate operation. Before the gate operation is performed, it may be necessary to sympathetically re-cool the qubit ions with another ion species [6]. Subsequently, these ions are moved to memory locations or other accumulators. This strategy always maintains a relatively small number of motional modes that must be considered and minimizes the problems of ion/laser-beam addressing using focused laser beams. Such arrays also enable highly parallel processing and ancilla qubit readout in a separate trapping region so that the logical ions are shielded from the scattered laser light.

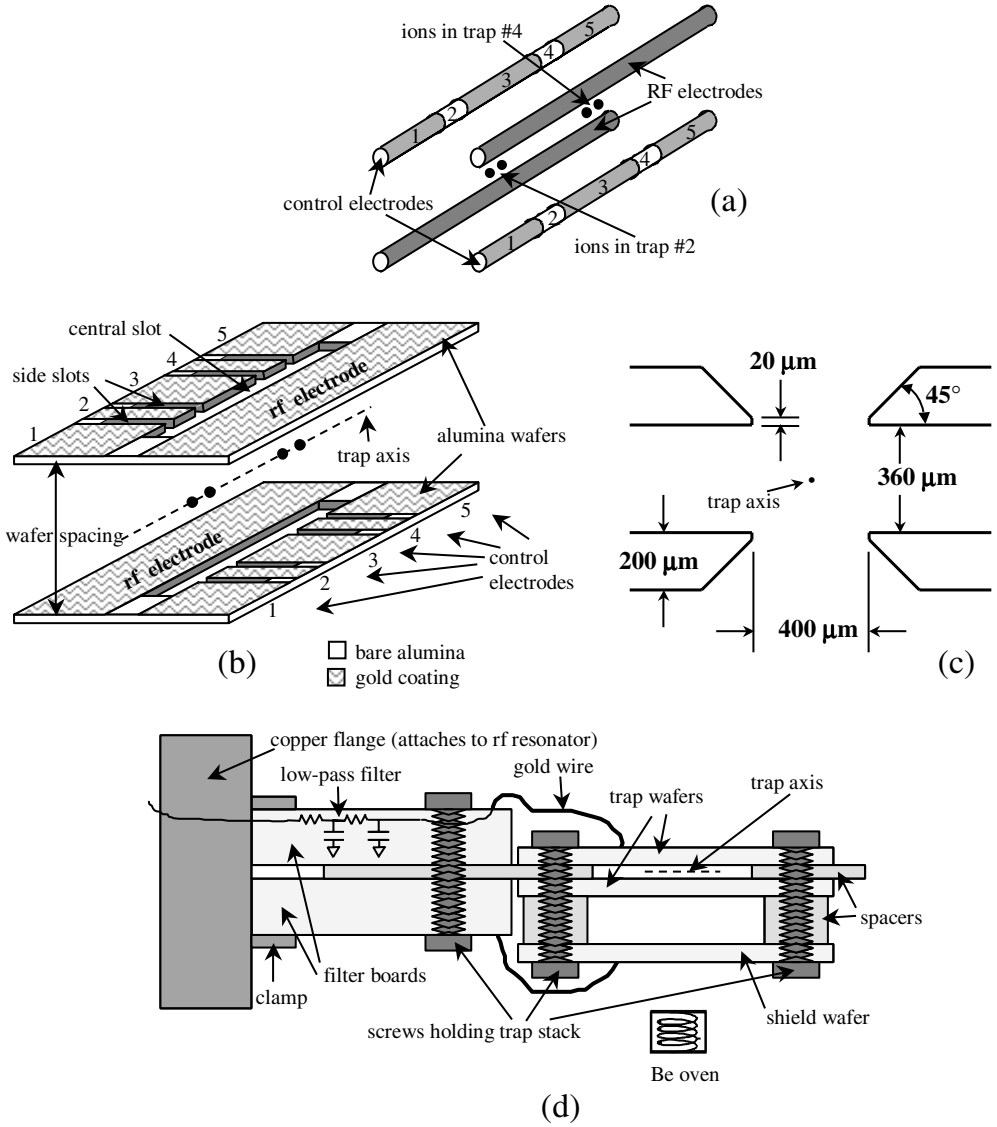

Figure 1. The 'dual' linear ion trap (drawings not to scale). (a) Idealized four-rod geometry; (b) wafer-stack implementation. The two trap wafers are spaced with two 360 μm thick alumina pieces (not shown) that are placed between them along the short edges. The pairs of control electrodes are numbered 1 through 5 for reference. The two trap locations, 2 and 4, shown in the figure are labelled by the electrode on which they are centred. The axial length of electrode 1 (2,3,4,5) is 1100 μm (400, 800, 400, 1100 μm). For 8.0 V applied to electrodes 1, 3, and 5 and 0.0 V applied to electrodes 2 and 4 the axial trap frequency in each trap was 2.9 MHz for a single $^9Be^+$ ion. The peak amplitude of the applied RF voltage was about 500 V. The RF drive frequency was 230 MHz. (c) Cross section of the trapping region; (d) schematic of the trap set-up including filter boards for low-pass filtering of the dc-electrodes and the extra board to shield the trap electrodes from Be deposition during loading.

2.1. 'Dual' linear ion trap

We have implemented some of the first steps towards realizing this scheme by moving ions in the 'dual' trap shown in figure 1. The trap was constructed from a stack of metallized 200 μm

thick alumina wafers. Laser-machined slots and gold traces created the desired electrode geometry [13]. Gold traces of 0.5 μm thickness were made with evaporated gold that was transmitted through a shadow mask and deposited on the alumina. Subsequently, an additional 3 μm of gold was electroplated onto the electrodes, resulting in electrode surfaces smooth at the 1 μm level. By smoothly changing the electric potentials on the control-electrode segments, we were able to translate our trapping potential and move ions between two locations (traps 2 and 4 in figure 1). Details of the experiments can be found in [13]. The key results were as follows.

(1) *Adiabatic transfer.* A single ion could be transferred between traps 2 and 4, a distance of 1.2 mm, in 25 μs while being kept in its ground state of motion. This time is approximately equal to the logic gate time, so if the transfer can be made somewhat faster in future work, the transfer time need not add a significant overhead in computational time.

(2) *Spin coherence.* By performing a two-zone Ramsey experiment with the two zones located at traps 2 and 4, we could show that no spin coherence was lost during transfer (to within our measurement precision of 0.5%).

(3) *Robustness.* No ion loss was observed during transfer (in any set of experiments, $>10^6$ transfers was typical).

(4) *Ion 'splitting'.* After placing two ions in a trap centred on electrode 3, by increasing the potential on these electrodes, a potential wedge was inserted between the ions, separating them into traps 2 and 4. The separation was accomplished with $\simeq$95% efficiency in a time of several milliseconds and the ions in their final respective wells had heated significantly ($\langle n \rangle \simeq 150$).

The heating that was observed upon separating ions was anticipated; to combat it, we expect that some sort of sympathetic re-cooling must be employed [6]. On the other hand, we believe the heating can be reduced and the separation time decreased substantially in future experiments. For example, the geometry of our dual trap is not well suited for separating ions. At the minimum centre-of-mass axial trap frequency during separation ($\sim$90 kHz) the ions are separated by about 50 μm. However, in the experiments reported here, we effectively insert an approximately 800 μm wide potential wedge between them at this point, making separation very sensitive to small field offsets. If we employ electrode dimensions where the distance from the ion to the nearest control electrode is about 50 μm, this should allow us to make the width of the wedge (electrode 3 in figure 1) approximately equal to this distance and make electrode voltage control much less stringent. Current efforts are therefore devoted to constructing smaller trap structures while maintaining high-quality electrode surfaces in order to suppress heating [13].

2.2. Sympathetic cooling

In the context of quantum computing, sympathetic cooling has been reported for like species (Ca^+) [14] and on isotopes of Cd^+ [15]. Recently we have sympathetically cooled $^9Be^+$ ions by Doppler cooling simultaneously trapped Mg^+ ions. We are currently exploring sympathetic ground state cooling using Raman transitions between the two $S_{1/2}$, $m = -1/2$ and $S_{1/2}$, $m = 1/2$ electronic ground states via the $P_{1/2}$ manifold. Successful implementation of this step would complete the in principle demonstrations of all ingredients necessary to implement quantum computing in the multiplexed trap architecture.

3. Coherent quantum control

The key entangling operation in the Cirac/Zoller scheme for QC, and the key to quantum gates between ions, is an operation that couples a spin qubit with the selected motion qubit. Assume that the spin qubit has a ground state (labelled $|\downarrow\rangle$) and a higher metastable state (labelled $|\uparrow\rangle$) that are separated in energy by $\hbar\omega_0$. Assume transitions between these levels can be excited with a focused laser beam. The interaction between an ion and the electric field of the laser beam can be written as

$$H_I(t) = -\tilde{\mathrm{d}}E = -\tilde{\mathrm{d}}E_0 \cos(k\tilde{z} - \omega_L t + \phi), \tag{1}$$

where $\tilde{\mathrm{d}}$ is the electric dipole operator, $\tilde{z}$ is the ion position operator for displacements from the ion's equilibrium position (expanded in terms of normal mode operators), k is the laser beam's k-vector (taken to be parallel to $\hat{z}$), ω_L is the laser frequency and ϕ is the phase of the laser field at the mean position of the ion. E is the laser's electric field, which is assumed to be classical. The dipole operator $\tilde{\mathrm{d}}$ is proportional to $\sigma^+ + \sigma^-$, where $\sigma^+ \equiv |\uparrow\rangle\langle\downarrow|$, $\sigma^- \equiv |\downarrow\rangle\langle\uparrow|$, and we take $\tilde{z} = z_0(a + a^\dagger)$, where a and $a^\dagger$ are the lowering and raising operators for the harmonic oscillator of the selected motional mode (frequency ω_z) and $z_0 \equiv \sqrt{\hbar/2m\omega_z}$ is the extension of the ground-state wavefunction. (Here, we assume all other z modes are cooled to and remain in their ground states, and for simplicity have neglected them in $\tilde{z}$.) In the Lamb–Dicke limit, where the extent of the ion's motion is much less than $\lambda/2\pi = 1/k$, we can write equation (1) (in the interaction frame, and making the rotating wave approximation [6]) as

$$H_I(t) \simeq \hbar\Omega\sigma^+ \mathrm{e}^{-\mathrm{i}(\omega_L - \omega_0)t + \phi}[1 + \mathrm{i}\eta(a\mathrm{e}^{-\mathrm{i}\omega_z t} + a^\dagger \mathrm{e}^{\mathrm{i}\omega_z t})] + \mathrm{H.c.} \tag{2}$$

Here, $\Omega \equiv E_0 d_{\downarrow\uparrow}/(2\hbar)$, where $d_{\downarrow\uparrow}$ is the electric-dipole matrix element between $|\downarrow\rangle$ and $|\uparrow\rangle$ and $\eta = kz_0$ is the Lamb–Dicke parameter ($\ll 1$ in the Lamb–Dicke limit).

For certain choices of ω_L, H_I is resonant and the spin and motion can be coupled efficiently. For example, when $\omega_L = \omega_0 - \omega_z$, $H_I \simeq \mathrm{i}\eta\hbar\Omega\sigma^+ a\mathrm{e}^{\mathrm{i}\phi} + \mathrm{h.c.}$ This is usually called the 'red-sideband' coupling and is formally equivalent to the Jaynes–Cummings Hamiltonian [16] from quantum optics. Here, $|\downarrow\rangle \rightarrow |\uparrow\rangle$ transitions are accompanied by $|n\rangle \rightarrow |n-1\rangle$ motional mode transitions. When $\omega_L = \omega_0 + \omega_z$, $H_I \simeq \mathrm{i}\eta\hbar\Omega\sigma^+ a^\dagger \mathrm{e}^{\mathrm{i}\phi} + \mathrm{h.c}$, the 'blue sideband', and $|\downarrow\rangle \rightarrow |\uparrow\rangle$ transitions are accompanied by $|n\rangle \rightarrow |n+1\rangle$ transitions. When $\omega_L = \omega_0$, $H_I \simeq \hbar\Omega\sigma^+\mathrm{e}^{\mathrm{i}\phi} + \mathrm{H.c.}$ and $|\downarrow\rangle \rightarrow |\uparrow\rangle$ transitions do not change n. These 'carrier' transitions are used to perform the single spin-qubit rotations.

In the $^9\mathrm{Be}^+$ experiments at NIST, two laser beams are used to drive two-photon stimulated-Raman transitions between two ground-state hyperfine spin-qubit levels ($|\downarrow\rangle \equiv |F = 2, m_F = -2\rangle$; $|\uparrow\rangle \equiv |F = 1, m_F = -1\rangle$). Here, k must be replaced by the difference Δk between k-vectors for the two Raman beams, ϕ is replaced by the phase difference between the laser beams, and $\Omega \propto E_1 E_2/\Delta$, where $E_{1,2}$ are the electric fields of the two beams and Δ is the nominal detuning of the beams from an allowed transition [6]. When the difference frequency of the Raman beams is tuned to resonance with the red or blue sidebands, entanglement between the ion and motion qubit occurs according to the coherent evolution

$$|\downarrow\rangle|n\rangle \rightarrow \cos(\Omega_{n,n'}t)|\downarrow\rangle|n\rangle - \mathrm{i}\mathrm{e}^{\mathrm{i}\phi}\sin(\Omega_{n,n'}t)|\uparrow\rangle|n'\rangle \tag{3}$$

and

$$|\uparrow\rangle|n\rangle \rightarrow -\mathrm{i}\mathrm{e}^{-\mathrm{i}\phi}\sin(\Omega_{n,n'}t)|\downarrow\rangle|n\rangle + \cos(\Omega_{n,n'}t)|\uparrow\rangle|n'\rangle. \tag{4}$$

Here, $n' = n \pm 1$ and $\Omega_{n,n'} \equiv \eta\Omega(n_>)^{1/2}$, where $n_>$ is the greater of n or n'. For each ion we are free to choose $\phi = 0$ but the phase of all operations on this ion must be referenced to

this choice[9]. Carrier transitions can also be described by expressions (3) and (4) where $n = n'$ and $\Omega_{n,n} = \Omega$. Since η must be kept large enough that the time to carry out an entangling operation is not too long, our interaction does not rigorously satisfy the Lamb–Dicke criterion. Therefore, we must add corrections to the expressions for the Rabi frequencies $\Omega_{n,n'}$. These correction factors, which can be called Debye–Waller factors [6], have been observed [17] and form the basis for a controlled-NOT (CNOT) gate described in what follows.

To initialize the qubits for each experiment, we use a combination of internal-state optical pumping (to pump to the $|\downarrow\rangle$ state) and sideband laser cooling to optically pump the motional modes to their ground states [18–21]. As in many atomic physics experiments, the observable in the ion-trap experiments is the ion's spin qubit state. We can efficiently distinguish $|\downarrow\rangle$ from $|\uparrow\rangle$ using a cycling transition to implement 'quantum jump' detection [22].

4. Quantum simulator

Treated as a small quantum processor, the trapped ion system can simulate the dynamics of other systems such as nonlinear optical beamsplitters [23]. One of the motivations behind Feynman's proposal for a quantum computer [24] was the possibility that one quantum system could efficiently simulate the behaviour of other quantum systems. This idea was verified by Lloyd [25] and further explored by Lloyd and Braunstein [26] for a conjugate pair of variables such as position and momentum of a quantum particle. Following this suggestion we show in what follows that coherent manipulation of the quantized motional and internal states of a single trapped ion using laser pulses can simulate the more general quantum dynamics of a single spin-1/2 particle in an arbitrary external potential. In addition to demonstrating the basic building blocks for simulating such arbitrary dynamics, we experimentally simulated the action of optical Mach–Zehnder interferometers with linear and nonlinear second- and third-order beamsplitters on number states. A number of optics experiments have exploited the second-order process of spontaneous parametric down conversion [27], which can be regarded as a nonlinear beamsplitter. By cascading this process, a fourth-order interaction has also recently been realized [28]. One difficulty in these experiments is the exponential decrease in efficiency as the order increases, necessitating data post-selection and long integration times. In the simulations reported here, nonlinear interactions were implemented with high efficiency, eliminating the need for data post-selection and thereby requiring relatively short integration times.

To realize a quantum computer for simulating a spin $s = 1/2$ particle of mass μ in an arbitrary potential, one must be able to prepare an arbitrary input state

$$|\Psi(m_s, z)\rangle = \sum_n (c_{\downarrow n}|\downarrow\rangle|n\rangle + c_{\uparrow n}|\uparrow\rangle|n\rangle), \tag{5}$$

where the particle's position wavefunction is expanded in energy eigenstates $|n\rangle$ of a suitable harmonic oscillator and $|m_s\rangle$ ($m_s \in \{\downarrow, \uparrow\}$) represent the spin eigenstates in a suitable basis. We have recently demonstrated a method to generate arbitrary states of the type given in equation (5) in an ion trap [29, 30]. The computer should then evolve the state according to an arbitrary Hamiltonian

$$H = \left[\frac{p^2}{2\mu} + V(z, m_s)\right] \simeq \sum_{n,m\leqslant n}^{N} (\alpha_{nm} I + \beta_{nm}\sigma_+ + \beta^*_{nm}\sigma_- + \gamma_{nm}\sigma_z) \times (\chi_{nm}(a^\dagger)^n a^m + \chi^*_{nm}(a^\dagger)^m a^n), \tag{6}$$

[9] In general, the laser phases (mod 2π) are not the same on each ion so the effective Bloch vectors for each ion are oriented differently in the lab frame. The choice $\phi = 0$ for each ion means that the spin coordinate frame for each ion is different.

where we require only that the potential $V(z, m_s)$ can be expanded as a power series in the harmonic oscillator ladder operators a and $a^\dagger$ and be approximated to arbitrary precision by a finite number of terms with maximum order N. The m_s are a set of observables in a general two-level Hilbert space that can all be mapped to a linear combination of the identity I and the Pauli matrices σ_j. The operators $\sigma_\pm$ are defined as $\sigma_\pm = \sigma_x \pm \mathrm{i}\sigma_y$, all β_{nm}, χ_{nm} are complex numbers, and all α_{nm}, γ_{nm} are real numbers.

Extending the interaction described in equation (2) the resonant interaction for Raman beam detuning $\Delta\omega = \epsilon\omega_0 + l\omega_z$ ($\epsilon = \{0, 1\}$, l integer) can be written (in the Lamb–Dicke limit) as [31]

$$H_{\epsilon l} = \hbar\Omega \mathrm{e}^{\mathrm{i}\phi}(\sigma_+)^\epsilon \left[\delta_{l,|l|}\frac{(\mathrm{i}\eta a)^{|l|}}{|l|!} + (1-\delta_{l,|l|})\frac{(\mathrm{i}\eta a^\dagger)^{|l|}}{|l|!}\right] + \mathrm{H.c.} \tag{7}$$

The coupling strength Ω is assumed to be small enough to resonantly excite only the lth spectral component. For $\epsilon = 1$ the internal state changes during the stimulated Raman transition and the interaction couples $|\downarrow\rangle|n\rangle \leftrightarrow |\uparrow\rangle|n+l\rangle$, while for $\epsilon = 0$ only motional states $|n\rangle \leftrightarrow |n+l\rangle$ are coupled with a strength independent of the internal state[10].

Following Lloyd and Braunstein [26], by nesting and concatenating sequences of $H_{\epsilon l}$ operations according to the relation[11]

$$\mathrm{e}^{-\frac{\mathrm{i}}{\hbar}H\delta t}\mathrm{e}^{-\frac{\mathrm{i}}{\hbar}H'\delta t}\mathrm{e}^{\frac{\mathrm{i}}{\hbar}H\delta t}\mathrm{e}^{\frac{\mathrm{i}}{\hbar}H'\delta t} = \mathrm{e}^{\frac{1}{\hbar^2}[H,H']\delta t^2} + \mathrm{O}(\delta t^3), \tag{8}$$

the set of operators $\{H_{01}, H_{02}, H_{03}, H_{10}, H_{11}, H_{12}, H_{13}\}$ is sufficient to efficiently generate arbitrary Hamiltonians. This conclusion is straightforward for the spin, since $\{\sigma_+, \sigma_-, \sigma_z\}$ are a complete basis of that algebra. For interactions that only involve the motion ($\epsilon = 0$) it follows from the fact that

$$[H_{02}, H_{03}] \propto \mathrm{i}\{\alpha a^\dagger a^2 + \alpha^*(a^\dagger)^2 a\} + \text{lower orders} \tag{9}$$

and

$$\begin{aligned}[\alpha a^\dagger a^2 + \alpha^*(a^\dagger)^2 a,\ &\beta(a^\dagger)^n a^m + \beta^*(a^\dagger)^m a^n] \\ &= (2m-n)[\alpha\beta(a^\dagger)^m a^{n+1} + \alpha\beta^*(a^\dagger)^n a^{m+1} - \mathrm{H.c.}] + \text{lower orders},\end{aligned} \tag{10}$$

so one can build up arbitrary orders in the effective Hamiltonian by recursive use of equation (8). Similar arguments hold for the set of $\{H_{1l}\}$ interactions, and by combining both types of interactions, the series expansion of the Hamiltonian in equation (6) can eventually be constructed.

Most of these interactions have been demonstrated in previous ion-trap experiments. H_{10} is usually called the carrier interaction, H_{01} and H_{02} are the coherent and squeeze drives respectively, and H_{11}, H_{12} are the first and second blue sidebands [32, 33]. The third-order interactions H_{03}, H_{13} have not been previously demonstrated. One of the experiments discussed in the following uses two H_{13} pulses, therefore demonstrating the feasibility of generating H_{03} as well[12].

As a demonstration of quantum simulation using a single trapped atom, we employ the interactions H_{11}, H_{12} and H_{13} to efficiently simulate a certain class of nth order optical beamsplitters described by Hamiltonians

$$B_n = \hbar\Omega_n[\mathrm{a}(\mathrm{b}^\dagger)^n + \mathrm{a}^\dagger(\mathrm{b})^n]. \tag{11}$$

[10] The coupling can be experimentally arranged to depend or not depend on the internal state, see [6].

[11] Note that equation (1) in [26] has a sign error in the right-hand side exponent.

[12] H_{13} and H_{03} both scale as $\eta^3\Omega$, and differ only by ω_0 in the Raman-detuning. Therefore successful implementation of H_{13} implies the feasibility of H_{03}.

Here a and b are the usual harmonic oscillators lowering operators for the two quantized light modes, Ω_n is the coupling strength, and we simulate the special case where the number of photons in mode a is 0 or 1 and $n = 1, 2$ or 3. Two such beamsplitters can be used to construct a Mach–Zehnder interferometer. The order $n = 1$ corresponds to the commonly used linear beamsplitter that is typically realized by a partially transparent mirror in experiments. Such interferometers can measure the relative phase of the two paths of the light fields that are split on the first beamsplitter and recombined on the second. The phase can be varied by changing a phase shifting element in one arm and detected (modulo 2π) by observing the interference fringes of the recombined fields. We restrict our attention to a pure number-state $|n = 1\rangle_{\mathrm{a}}$ impinging on the first beamsplitter from mode a and a vacuum state $|n = 0\rangle_{\mathrm{b}}$ from mode b. After propagating the input state through the first beamsplitter with Ω_n adjusted to give equal amplitude between the two paths in the output superposition, the state becomes

$$|1\rangle_{\mathrm{a}}|0\rangle_{\mathrm{b}} \rightarrow \frac{1}{\sqrt{2}}(|1\rangle_{\mathrm{a}'}|0\rangle_{\mathrm{b}'} + |0\rangle_{\mathrm{a}'}|n\rangle_{\mathrm{b}'}). \tag{12}$$

Phase shifters in optical interferometers alter a classical-like coherent state $|\alpha\rangle$ to one that is shifted to $|\alpha \mathrm{e}^{\mathrm{i}\phi}\rangle$. For the state in equation (12) this phase shift corresponds to $|n\rangle \rightarrow \mathrm{e}^{\mathrm{i}n\phi}|n\rangle$ for a number state, leading to

$$\frac{1}{\sqrt{2}}(|1\rangle_{\mathrm{a}'}|0\rangle_{\mathrm{b}'} + |0\rangle_{\mathrm{a}'}|n\rangle_{\mathrm{b}'}) \rightarrow \frac{1}{\sqrt{2}}(|1\rangle_{\mathrm{a}'}|0\rangle_{\mathrm{b}'} + \mathrm{e}^{\mathrm{i}n\phi}|0\rangle_{\mathrm{a}'}|n\rangle_{\mathrm{b}'}). \tag{13}$$

The second beamsplitter recombines the two field modes leading to an average probability of

$$\langle \hat{n}_{\mathrm{a}''} \rangle = \tfrac{1}{2}[1 - \cos(n\phi)] \tag{14}$$

for detecting one photon in the corresponding output arm.

We have experimentally simulated the nonlinear beamsplitter of equation (11) using a single trapped ion. The operator a is replaced by σ^+. These operators (and also their respective Hermitian conjugates) are not strictly equivalent, but their action is the same as long as we restrict our attention to situations that never leave the $\{|0\rangle_{\mathrm{a}}, |1\rangle_{\mathrm{a}}\}$ subspace. The simulated linear and nonlinear interferometers fulfil this restriction, as long as the input state is $|1\rangle_{\mathrm{a}}|0\rangle_{\mathrm{b}}$. The optical mode with lowering operator b is replaced by the equivalent harmonic oscillator mode of motion along one axis in the trap, with number states $|n\rangle$.

Starting from the $|1\rangle_{\mathrm{a}}|0\rangle_{\mathrm{b}}$ state we used Raman transitions to drive a $\pi/2$-pulse on the ion's nth blue sideband ($H_I \propto \sigma^+(b^\dagger)^n + \mathrm{H.c.}$), creating the state $(|1\rangle_{\mathrm{a}'}|0\rangle_{\mathrm{b}'} + |0\rangle_{\mathrm{a}'}|n\rangle_{\mathrm{b}'})/\sqrt{2}$. A phase shift $\phi = \Delta\omega_z\, t$ was then introduced by adiabatically switching the potential of the trap endcaps to a different value for time t, thus changing the motional frequency by a fixed amount $\Delta\omega_z$. After a second $\pi/2$-pulse on the nth sideband we measured the probability $\langle n_{\mathrm{a}''} \rangle$ for the ion to be in $|1\rangle_{\mathrm{a}}$, that simply corresponds to the probability of finding the ion in $|\downarrow\rangle$ in our simulation. The interference fringes created by sweeping t are shown in figure 2. The final state of the ion oscillated approximately between $|1\rangle_{\mathrm{a}''}$ and $|0\rangle_{\mathrm{a}''}$ as t was varied, with frequency $n\Delta\omega_z$.

The interactions used in the interferometers demonstrate that in principle coherent stimulated-Raman transitions on a single trapped atom can be used to simulate a wide class of Hamiltonians of a spin-1/2 particle in an arbitrary external potential. This system can also be used to simulate other physical dynamics, as our demonstration of nth order nonlinear optical beamsplitters acting in a restricted Hilbert space shows. As a practical matter, the second- and third-order beamsplitters demonstrated here give increased sensitivity for diagnosing motional frequency fluctuations in the trapped-ion system. With anticipated improvements in motional state coherence [13], it should be possible to simulate more complicated Hamiltonians. An exciting possibility is that these studies might eventually uncover some as-yet-unseen fundamental source of decoherence (see, for example, [34]).

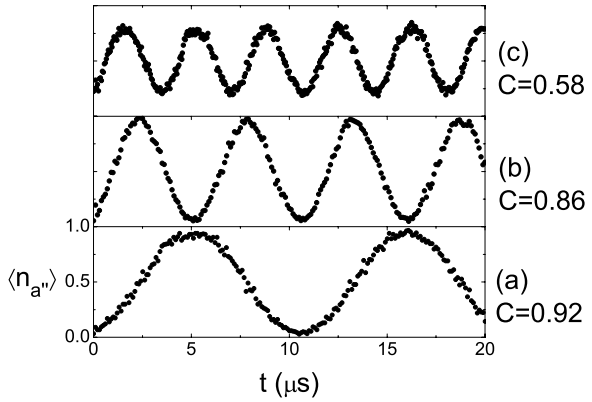

Figure 2. Interference fringes for simulated interferometers: (a) of order $n = 1$ (the integration time per data point was 0.50 s); (b) $n = 2$, (0.53 s) and (c) $n = 3$, (0.63 s). $\langle n_{a''} \rangle$ is the probability of finding the ion in $|1\rangle_{a''}$, while t is the time for which the trap frequency was shifted by $\Delta\omega_z$, directly proportional to the phase shift $\phi = \Delta\omega_z t$. The frequency of the fringes increases linearly with order n. C is the observed contrast of the fringes.

5. Gates

Equations (3) and (4) illustrate the basic source of entanglement in ion experiments from which universal logic gates have been constructed. For example, a CNOT and π-phase gate between the motion and spin qubit for a single ion have been realized at NIST [6, 35]. Also, using the scheme suggested by Sørensen and Mølmer [36, 37] and Solano *et al* [38], the NIST group realized a universal gate between two spin qubits [39, 40]. Compared to the original Cirac and Zoller gate [1], this last gate has the advantages that:

(1) laser-beam focusing (for individual ion addressing) is not required,
(2) it can be carried out in one step,
(3) it does not require the use of an additional internal state, and
(4) it does not require precise control of the motional state (as long as the Lamb–Dicke limit is satisfied).

From this gate, a CNOT gate can be constructed [36]. In recent experiments, we have significantly reduced motional heating [13] allowing us to explore new types of gates and improve the fidelity of the operations.

5.1. Controlled-NOT wavepacket gate

Recently, we have experimentally demonstrated [41] a new kind of CNOT gate between the motion qubit (control bit) and spin qubit (target bit) that was proposed in [42]. This gate uses carrier transitions and relies on Debye–Waller correction factors to provide the conditional dynamics for the gate. Including these correction factors [6], the n-dependent carrier Rabi frequencies become

$$\Omega_{n,n} = \Omega e^{-\eta^2/2} L_n(\eta^2), \tag{15}$$

where $L_n(X)$ is the Laguerre polynomial of order n. For the lowest three values of n, we have

$$L_0(\eta^2) = 1, \qquad L_1(\eta^2) = 1 - \eta^2, \qquad L_2 = 1 - 2\eta^2 + \eta^4/2. \tag{16}$$

To construct the CNOT gate we could, for example, configure the experiment to make $\eta^2 = 1/2$ and drive the carrier transition for a time such that $\Omega_{0,0}t = \pi$ [42]. We find the state transformations (choosing $\phi = 0$) $|\downarrow\rangle|0\rangle \rightarrow -|\downarrow\rangle|0\rangle$, $|\uparrow\rangle|0\rangle \rightarrow -|\uparrow\rangle|0\rangle$, $|\downarrow\rangle|1\rangle \rightarrow -i|\uparrow\rangle|1\rangle$, and $|\uparrow\rangle|1\rangle \rightarrow -i|\downarrow\rangle|1\rangle$. Up to phase factors that can be corrected by single-ion qubit rotations (or accounted for in software[13]), this gate is the CNOT gate: if the control bit is a 1, the spin qubit flips, if the control bit is a 0, the spin qubit remains unchanged. In the experiment, the single-ion oscillation frequency and Lamb–Dicke parameter η are related through $\omega_z/2\pi$ (MHz) $= 0.453/\eta^2$, so to carry out the gate we want $\omega_z/2\pi = 0.906$ MHz. Because the ion heating was fairly strong at this relatively low frequency, we chose $\eta^2 = 0.129$ which gave $\omega_z/2\pi = 3.51$ MHz and relatively small heating. For the motional qubit states we chose $|n = 0\rangle$ and $|n = 2\rangle$ so that the chosen value of η gave $\Omega_{0,0}/\Omega_{2,2} = 4/3$. Therefore, by choosing the interaction time such that $\Omega_{0,0}t = 2\pi$, we also realize the desired CNOT gate. Compared to the previously realized CNOT gate between motion and spin [35] this gate has the following advantages:

(1) it requires one step instead of three,
(2) it does not require an auxiliary internal state, and
(3) it is immune to Stark shifts caused by coupling to 'spectator' states [6] (here, Stark shifts from coupling to non-resonant sideband transitions).

This gate is fundamentally different from previously demonstrated gates in that it relies on the wavepacket nature of the ions. To obtain the correct interaction with the laser, we must average the laser field over the extent of the ion's wavepacket rather than assuming it is a point particle.

5.2. Geometrical phase gate between two ions

In a separate experiment, we realized a phase gate between two spin qubits [43] that carried out the state transformations: $|\downarrow\rangle|\downarrow\rangle \rightarrow |\downarrow\rangle|\downarrow\rangle$, $|\downarrow\rangle|\uparrow\rangle \rightarrow e^{i\pi/2}|\downarrow\rangle|\uparrow\rangle$, $|\uparrow\rangle|\downarrow\rangle \rightarrow e^{i\pi/2}|\uparrow\rangle|\downarrow\rangle$, and $|\uparrow\rangle|\uparrow\rangle \rightarrow |\uparrow\rangle|\uparrow\rangle$. Combined with single-bit rotations, this operation can, among others, yield either a π-phase gate or the CNOT operation. The gate relies, in part, on the properties of motional states as they are displaced in phase space. For a particular motional mode, the displacement operator can be written [44]

$$D(\alpha) = e^{\alpha a^\dagger + \alpha^* a}, \tag{17}$$

where α is a complex number. For two successive displacements we have

$$D(\alpha)D(\beta) = D(\alpha + \beta)e^{iIm[\alpha\beta^*]}. \tag{18}$$

Now consider constructing a closed path in phase space so that the state returns to its original position. We can derive the effects of this transformation by constructing the closed path from a series of successive applications of equation (18) with infinitesimal displacements. The net effect is that the mode wavefunction acquires an overall phase shift that depends on the area enclosed by the path.

The second element required for the gate is to make the path area spin dependent. This is accomplished by making the displacement in phase space with a spin-dependent optical dipole force as was done in previous experiments [45, 46]. To implement this gate on two ions, the

[13] Neglecting the overall minus sign, the transformation looks like the desired CNOT operation followed by a $\pi/2$ phase shift ($i = e^{i\pi/2}$) on the $|1\rangle$ state of the motion qubit. This phase shift can be removed by shifting the phase of the relevant laser oscillator for the next operation on the motion qubit.

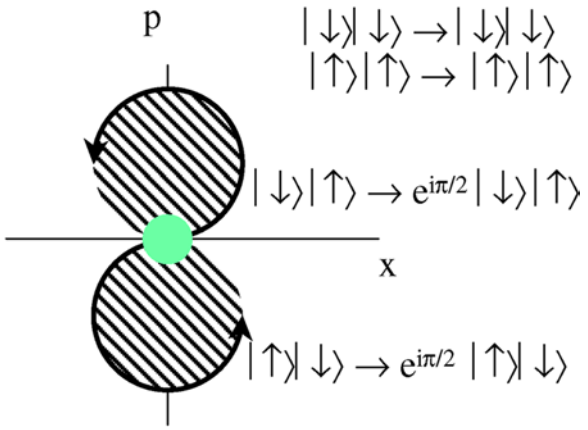

Figure 3. Schematic representation of the displacements of the axial stretch-mode amplitude in phase space for the four basis states of the two spin qubits. The detuning and amplitude of the displacements are chosen to give a $\pi/2$ phase shift on the $|\downarrow\rangle|\uparrow\rangle$ and $|\uparrow\rangle|\downarrow\rangle$ states while the $|\downarrow\rangle|\downarrow\rangle$ and $|\uparrow\rangle|\uparrow\rangle$ states are unaffected because the optical dipole forces for these states do not couple to the stretch mode.

(This figure is in colour only in the electronic version)

Raman transition beams were separated in frequency by $\sqrt{3}\omega_z + \delta$, where $\sqrt{3}\omega_z$ is the stretch-mode frequency for two ions and δ is a small detuning (below). The separation of the ions was adjusted to be an integer multiple of $2\pi/\Delta k$ so that the optical-dipole force (from the 'walking' standing wave) on each ion was in the same direction if the ions were in the same spin state but, due to the choice of laser polarizations, in opposite directions if the spin states were different. This had the effect that the application of the laser beams to the $|\downarrow\rangle|\uparrow\rangle$ and $|\uparrow\rangle|\downarrow\rangle$ states caused excitation on the stretch mode but the $|\downarrow\rangle|\downarrow\rangle$ and $|\uparrow\rangle|\uparrow\rangle$ states were unaffected. The detuning δ and duration of the displacement pulses were chosen to make one complete (circular) path in phase space with an area that gave a phase shift of $\pi/2$ on the $|\downarrow\rangle|\uparrow\rangle$ and $|\uparrow\rangle|\downarrow\rangle$ states. This is shown schematically in figure 3. The total operation acts like the product of an operator that applies a $\pi/2$ phase shift to the $|\uparrow\rangle$ state on each ion separately (a non-entangling gate) and a $-\pi$ phase gate. The effects of the first can be removed by single-ion qubit rotations (or accounted for in software) leaving a $-\pi$ phase gate. The origin of this phase gate can also be viewed as a particular case of the more general formalism developed in [36, 47, 48]. Compared to the original Cirac and Zoller gate [1], this shares the same advantages as the Sørensen and Mølmer [36, 37] gate realized in [39]. In addition, the internal states of the gated qubits remain untouched, since the acquired phase is of purely geometrical origin.

5.3. Perspective

The obstacles to building a large-scale quantum computer appear to be technical rather than fundamental. However, by anyone's reckoning, realizing such a device will be extremely difficult and take a long period of time. Therefore, it is important to establish some intermediate goals upon which projections about scaling can be made. A couple of the more important interim goals appear to be the following.

(1) Error correction [49]. Here, a superposition state of a physical spin qubit is encoded into a 'logical' qubit composed of several entangled physical qubits. Measurements of a subset of these bits allows one to correct for phase or bit-flip errors on any of the physical qubits.

By repeating the encoding and measurement process, the logical bit can be preserved while under the influence of decoherence[14].

(2) High-fidelity logic operations. The probability of an error generated by logic operations must be less than 10^{-4} or smaller [8] in order for error correction to enable arbitrarily long computations. For example, laser beam intensity stability is crucial; also, spontaneous emission can be an important limitation [50]. For the case of stimulated-Raman transitions, we desire a large ratio of fine-structure splitting to excited-state lifetime to suppress spontaneous emission. This rules out $^9Be^+$ as the ultimate qubit and favours ions such as Sr^+, Cd^+ [15], or Hg^+ [51].

(3) Simulation of other quantum systems. Even the simulation of the behaviour of a relatively modest number of 50 qubits would need a classical memory of about 32 TB, beyond the capability of existing computers. On the other hand this number of qubits would, among other examples, allow for the simulation of models for high-temperature superconductors [52]. Small errors in the simulator operations would not be too critical, since they merely translate into a finite temperature that still could be below the temperature of the anticipated transition to the superconducting phase in the simulated system.

6. Fundamental tests, measurement applications

The ability to coherently manipulate entangled quantum states, at least on a small scale, has enabled some demonstrations and tests of quantum mechanical principles that would otherwise remain as gedanken experiments. For trapped ions, nonclassical motional states have been engineered by use of the basic elements of quantum logic [17] and their properties determined through tomographic methods [53]. Motional Schrödinger-cat states have been generated [45] and the scaling of their decoherence based on the size of the cat state has been verified [46, 54]. A scheme for the generation of arbitrary motional states has recently been demonstrated on a single ion [30]. Entanglement of up to four separate ions has been generated deterministically ('on demand') [39, 55] without the need for post-selection as in experiments using parametric down conversion of photons. This enabled the first experiment showing a violation of Bell's inequalities (on massive particles) while defeating the 'detection loophole' [56].

A goal of the NIST experiments has been to use entanglement ('spin-squeezing') to increase the signal-to-noise ratio in spectroscopy and atomic clocks [57, 58]. An experiment on two ions has recently shown such squeezing [59] and although not yet of practical use, we could show that the squeezing that was obtained led to a signal-to-noise ratio higher than could possibly be attained without entanglement. Simple quantum processing might also be used to aid in quantum measurement readout with potential applications to mass spectroscopy [60] and frequency standards [61].

Acknowledgments

This work was supported by the US National Security Agency (NSA) and Advanced Research and Development Activity (ARDA) under contract no MOD-7171.00, the US Office of Naval Research (ONR) and the US National Reconnaissance Office (NRO). The paper is a contribution of NIST and not subject to US copyright.

[14] Passive means of fighting decoherence such as decoherence-free-subspaces have recently been demonstrated for ions [40] and might also be employed directly in future QC [7].

References

[1] Cirac J I and Zoller P 1995 *Phys. Rev. Lett.* **74** 4091
[2] Jaksch D *et al* 2000 *Phys. Rev. Lett.* **85** 2208
[3] DiVincenzo D P 1995 *Phys. Rev.* A **51** 1015
[4] Barenco A *et al* 1995 *Phys. Rev.* A **52** 3457
[5] DiVincenzo D P 2001 *Scalable Quantum Computers* ed S L Braunstein and H K Lo (Berlin: Wiley) pp 1–13
[6] Wineland D J *et al* 1998 *J. Res. Natl Inst. Stand. Tech.* **103** 259
[7] Kielpinski D, Monroe C and Wineland D J 2002 *Nature* **417** 709
[8] Steane A M and Lucas D M 2000 *Scalable Quantum Computers* ed S L Braunstein, H K Lo and P Kok (Berlin: Wiley) pp 69–88
[9] Cirac J I, Zoller P, Kimble H J and Mabuchi H 1997 *Phys. Rev. Lett.* **78** 3221
[10] Pellizzari T 1997 *Phys. Rev. Lett.* **79** 5242
[11] DeVoe R G 1998 *Phys. Rev.* A **58** 910
[12] Cirac J I and Zoller P 2000 *Nature* **404** 579
[13] Rowe M A *et al* 2002 *Quant. Inform. Comput.* **2** 257
[14] Rohde H *et al* 2001 *J. Opt. B: Quantum Semiclass. Opt.* **3** S34
[15] Blinov B B *et al* 2002 *Phys. Rev.* A **65** 040304
[16] Raimond J M, Brune M and Haroche S 2001 *Rev. Mod. Phys.* **73** 565
[17] Meekhof D M *et al* 1996 *Phys. Rev. Lett.* **76** 1796
[18] Roos C *et al* 1999 *Phys. Rev. Lett.* **83** 4713
[19] Diedrich F *et al* 1989 *Phys. Rev. Lett.* **62** 403
[20] Monroe C *et al* 1995 *Phys. Rev. Lett.* **75** 4714
[21] Roos C F *et al* 2000 *Phys. Rev. Lett.* **85** 5547
[22] Blatt R and Zoller P 1988 *Eur. J. Phys.* **9** 250
[23] Leibfried D *et al* 2002 *Preprint* quant-ph/0209028
[24] Feynman R P 1985 *Int. J. Theor. Phys.* **21** 467
[25] Lloyd S 1996 *Science* **273** 1073
[26] Lloyd S and Braunstein S L 1999 *Phys. Rev. Lett.* **82** 1784
[27] For an overview see for example
Tittel W and Weihs G 2001 *Quant. Int. Comput.* **1** 3
[28] Lamas-Linares A, Howell J C and Bouwmeester D 2001 *Nature* **412** 887
Howell J C, Lamas-Linares A and Bouwmeester D 2002 *Phys. Rev. Lett.* **88** 030401
[29] Law C K and Eberly J H 1996 *Phys. Rev. Lett.* **76** 1055
[30] Ben-Kish A *et al* 2002 *Preprint* quant-ph/0208181
[31] Wineland D J *et al* 1998 *Phys. Scr.* T **76** 147
[32] Meekhof D M *et al* 1996 *Phys. Rev. Lett.* **76** 1796
[33] Leibfried D *et al* 1997 *J. Mod. Opt.* **44** 2485
[34] Leggett A J 1999 *Phys. World* **12** 73
[35] Monroe C *et al* 1995 *Phys. Rev. Lett.* **75** 4714
[36] Sørensen A and Mølmer K 1999 *Phys. Rev. Lett.* **82** 1971
[37] Sørensen A and Mølmer K 2000 *Phys. Rev.* A **62** 02231
[38] Solano E, de Matos Filho R L and Zagury N 1999 *Phys. Rev.* A **59** 2539
[39] Sackett C A *et al* 2000 *Nature* **404** 256
[40] Kielpinski D *et al* 2001 *Science* **291** 1013
[41] DeMarco B *et al* 2002 *Preprint* quant-ph/0208180
[42] Monroe C *et al* 1997 *Phys. Rev.* A **55** R2489
[43] Leibfried D *et al* 2002 in preparation
[44] Walls D F and Milburn G J 1994 *Quantum Optics* 1st edn (Berlin: Springer)
[45] Monroe C, Meekhof D M, King B E and Wineland D J 1996 *Science* **272** 1131
[46] Myatt C J *et al* 2000 *Nature* **403** 269
[47] Milburn G J, Schneider S and James D F 2000 *Scalable Quantum Computers* ed S L Braunstein, H K Lo and P Kok (Berlin: Wiley) pp 31–40
[48] Wang X, Sørensen A and Mølmer K 2001 *Phys. Rev. Lett.* **86** 3907
[49] Nielsen M A and Chuang I L 2000 *Quantum Computation and Quantum Information* 1st edn (Cambridge: Cambridge University Press)
[50] Plenio M B and Knight P L 1997 *Proc. R. Soc.* A **453** 2017
[51] Wineland D J 2002 *Proc. Fermi School on Quantum Computation; Nuovo Cimento* at press

[52] Cirac I J 2002 Private communication
[53] Leibfried D *et al* 1996 *Phys. Rev. Lett.* **77** 4281
[54] Turchette Q A *et al* 2000 *Phys. Rev.* A **62** 053807
[55] Turchette Q A *et al* 1998 *Phys. Rev. Lett.* **81** 1525
[56] Rowe M A *et al* 2001 *Nature* **409** 791
[57] Wineland D J *et al* 1992 *Phys. Rev.* A **46** R6797
[58] Bollinger J J, Itano W M, Wineland D J and Heinzen D J 1996 *Phys. Rev.* A **54** R4649
[59] Meyer V *et al* 2001 *Phys. Rev. Lett.* **86** 5870
[60] Heinzen D J and Wineland D J 1990 *Phys. Rev.* A **42** 2977
[61] Wineland D J *et al* 2002 *Proc. 6th Symp. on Frequency Standards and Metrology* ed P Gill (Singapore: World Scientific) pp 361–8